Thermochimica Acta, 232 (1994) 249–260
Elsevier Science B.V., Amsterdam
SSDI 0040-6031(93)01399-N

Spectral and thermal analyses of small structural shifts in some highly symmetric polycyclic aryl derivatives of cyclotriphosphazatriene

Moein B. Sayed

Chemistry Department, Qatar University, Doha-2713 (Qatar)

(Received 8 April 1993; accepted 10 June 1993)

Abstract

Small structural shifts are induced in cyclotriphosphazatriene by symmetric substitution of its hexachloro derivative with analogous aryl derivatives, namely hexaphenyl, trisbiphenyl, trisnaphthyl and trisfluorene. These shifts are structurally probed by spectral analysis and thermally sensed by differential thermal analysis. Except for the fluorene derivative, which shows a coplanar ring structure, the other derivatives presume a molecular configuration in which the aryl rings are located in a plane perpendicular to the phosphazene ring. Such a perpendicular configuration facilitates strong intramolecular hydrogen bonding, which associates the aryl π-bonding electrons with the protonated phosphazene ring, which is not possible for the fluorene coplanar structure. The intramolecular association follows a typical order of the molecular resonance induced in these polycyclic phosphazenes: phenyl > biphenyl > naphthyl > fluorene.

Various spectral evidence consistently support the proposed order of molecular resonance and intramolecular association. Also, various thermodynamic parameters of solid state and solid–liquid phase transitions consistently confirm that these polycyclic phosphazenes are structurally strained. However, the intramolecular association and molecular resonance play a significant role in stabilising the molecular structure against strain so that the thermal data reveal thermodynamic parameters reflecting the same order for the molecular thermal stability.

INTRODUCTION

In a recent investigation [1], spectral analysis was applied as a molecular probe to studying the structural shifts which are induced in the D_{3h}-symmetric hexachlorocyclotriphosphazatriene upon lowering the molecular symmetry to the C_{2v}-symmetric bis- and tetrakis-phenyl derivatives, and also on reverting to the D_{3h}-symmetric hexaphenyl derivative. Except for the highly symmetric phenyl derivative, all the derivatives experienced an endothermic solid–liquid phase transition, which is dependent on the molecular resonance induced by the phenyl substituent. The hexaphenyl derivative, in addition, revealed another endothermic solid–solid phase transition, which is characterised by lower T_c, C_p, ΔH and E^* values. The

latter solid state phase transition was attributed to a thermally enhanced structural shift from distorted C_{3v} to the higher symmetry D_{3h}. Such a structural shift, although observed spectrally [2–5], has not yet been thermally revealed for the less strained hexachloro derivative of this cyclic phosphazene.

In this work, spectral and thermal analyses were applied in the study of the effect of slight structural shifts in analogous polycyclic aryl derivatives, namely trisbiphenyl, trisnaphthyl and trisfluorene, with reference to the effects of the hexaphenyl and hexachloro derivatives of cyclotriphosphazatriene on the thermodynamics of their solid state and solid–molten phase transitions.

EXPERIMENTAL

The materials used were hexachlorocyclotriphosphazatriene from Nippon Soda Co. Ltd., anhydrous aluminium chloride from Fluka, and the aryl derivatives of biphenyl, naphthalene, fluorene and benzene from BDH.

The arylation method of Friedel-Craft was applied in dry toluene to the hexachloro derivative for the synthesis of the present derivatives. The trisbiphenyl derivative (m.p. 473 K) was formed in higher yield and at a faster rate than for the trisnaphthyl (m.p. 465 K) and the trisfluorene (m.p. 393 K) derivatives, but less than for the hexaphenyl derivative (m.p. 510 K). Because of the high basicity induced in the phosphazene ring of the phenyl, biphenyl and naphthyl derivatives, the phosphazene ring was unavoidably protonated by the HCl gas generated during the synthesis.

The IR measurements were performed in the solid state, using the KBr disc technique and a Nicholet FT-IR 510P spectrometer. The UV spectra were recorded in 10^{-4} M ethanol using a Beckman Du-70 spectrophotometer. The ^{1}H-NMR spectra were measured in deuterated trifluoroacetic acid, using a 100 MHz Bruker spectrometer. The DTA thermograms were measured in air for solid samples weighing 30 mg, using a Shimadzu TA 30 thermal analyser in the temperature range of 300–600 K. The temperature rise was controlled at 10 K min^{-1}. The thermal data were treated as described elsewhere [6].

RESULTS AND DISCUSSION

Infrared spectra

The band frequencies and proposed assignments are shown in Table 1. The high-frequency spectrum of the hexachloro derivative (Fig. 1, curve

TABLE 1

IR band frequency (cm^{-1}) and assignment [a] (4000–200 cm^{-1}) of the cyclotriphosphazatriene derivatives

	Polycyclic aryl derivative of cyclotriphosphazatriene				
	Phenyl	Biphenyl	Naphthyl	Fluorene	Chloro
Phosphazene ring deformations	511s 550s	519m 553m	528m 575m	470m 555w–m	
Stretching $\equiv PCl_2$ sym. asym.					529s 603s
Out-of-plane C–H bending	694s 723m 748m	698m 739w–m 760m	698m 762m 785m	690w 733w 766w	
Out-of-plane N^+–H bending	941br	934br	950br		
In-plane C–H bending	1000w 1028w	1000w 1020w	1000w 1025w	1000w 1020w	
Phosphazene ring stretching	1124s 1152s 1294s	1125s 1179s 1221s	1120s 1182s 1215s	1120m 1177s 1221s	1221s
In-plane C–H cyclic				1408w	
Aryl ring stretching	1439s 1481w–m 1590w–m	1448w 1483w–m 1599m	1449m–s 1483sh 1600s	1451w–m 1602w–m	
In-plane N^+–H bending	1620br	1620br	1620br		
Stretching N^+–H (associated)	2620br	2670br	2720sh		
Stretching C–H, free	2920sh	2922w–m	2922m	2921w–m	
Stretching C–H mode	3054w–m	3053w–m	3052w–m	3050w–m	
Stretching N^+–H, free	3365br	3365br	3365br		

Key: w, weak; m, medium; s, strong; sh, shoulder; and br, broad.

[a] Band assignment is made as based on spectral correlation with previously published relevant data [11, 12].

C) shows no absorptions, except for a number of non-fundamental modes near 2000 cm^{-1}. The other derivatives (Fig. 1, curves F, N, B, P) consistently show a characteristic aryl C–H stretching band at 3052 ± 2 cm^{-1}. In addition, another less bonded C–H stretch is shown at a lower frequency of 2922 cm^{-1}. On both the higher and lower frequency sides, two broad absorptions appear at 3365 and 2670 ± 50 cm^{-1} (Fig. 1, curves N, B, P) which are attributed to protonated phosphazene N^+–H stretching modes [7]. The less bonded C–H mode may contribute to the strong intramolecular association of the aryl rings with the protonated

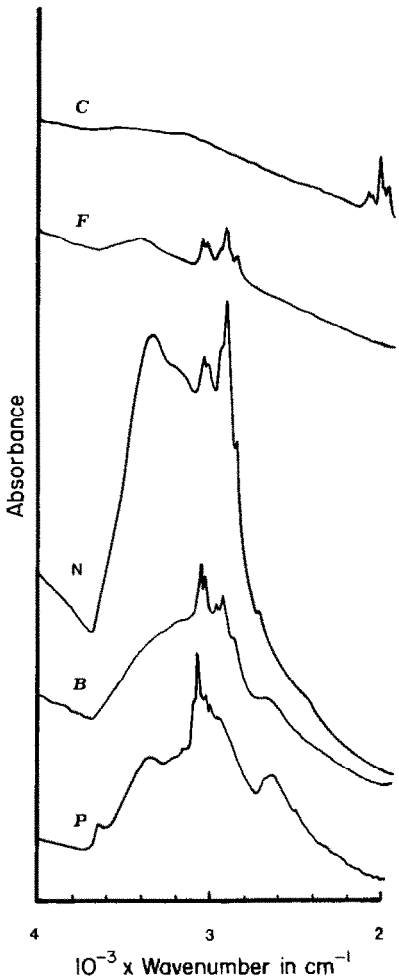

Fig. 1. IR spectra (4000–2000 cm^{-1}) of: C, hexachloro; F, trisfluorene; N, trisnaphthyl; B, trisbiphenyl; and P, hexaphenyl cyclotriphosphazatrienes.

phosphazene ring. Such high-frequency data demonstrate a higher association for the phenyl derivative than for the biphenyl derivative, which is higher than for the naphthyl derivative; no evidence of association is shown for the fluorene derivative.

Figure 2 illustrates the mid- to low-frequency IR spectra. Complementary to the high-frequency data, this figure reveals broad bands at 1620 and $940 \pm 10\ cm^{-1}$ due to the in-plane and out-of-plane N^+–H deformations of the protonated phosphazene ring [7], respectively. The strong association is maximum for the phenyl derivative (Fig. 2, curve P), less for the biphenyl derivative (Fig. 2, curve B) and lowest for the naphthyl derivative (Fig. 2, curve N). The band splitting in the phosphazene ring breathing mode at 1221 cm^{-1} increases with the geminal substitution and shifts to higher

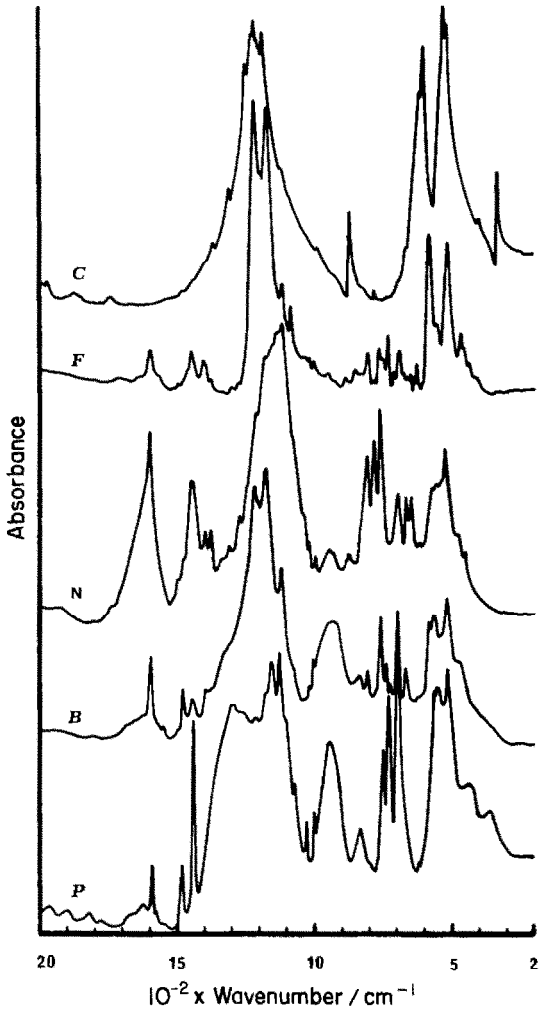

Fig. 2. IR spectra (2000–200 cm^{-1}) of the cyclotriphosphazatriene derivatives. Symbols as in Fig. 1.

frequencies with the more electronegative or mesomeric substituent [8–10]. Both spectral shifts are shown to follow the order phenyl > biphenyl > naphthyl > fluorene. The band frequency of the dominant aryl ring stretching modes also increases in the same order (Table 1) as the molecular resonance induced in these polycyclics.

At variance with the other aryl derivatives, and consistent with the hexachloro derivative (Fig. 2, curve C), the fluorene derivative (Fig. 2, curve F) shows evidence of persisting $\equiv PCl_2$ stretching modes at 517 and 582 cm^{-1}, which are shifted to lower frequencies with respect to those of the hexachloro derivative, probably because of the increased molecular resonance. This, together with the evidence of cyclic C–H in-plane bending

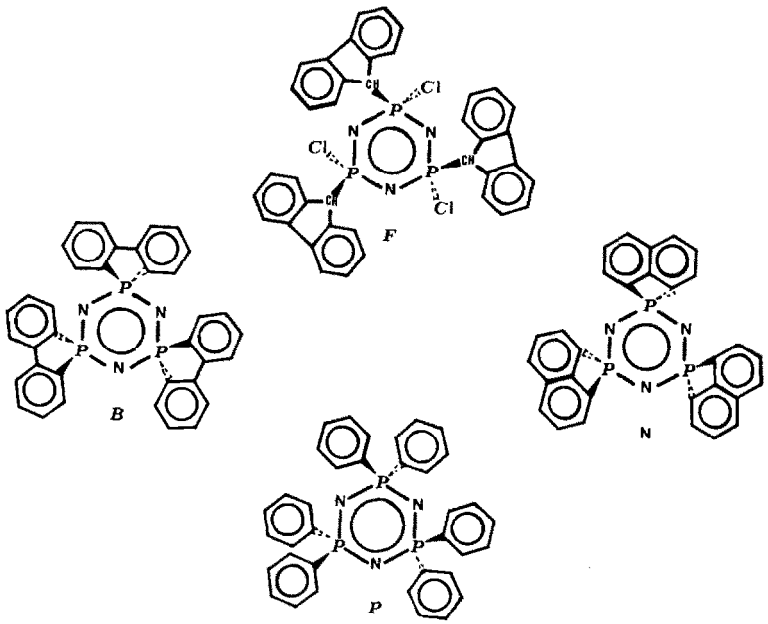

Scheme 1. A proposed molecular configuration of: B, trisbiphenyl; F, trisfluorene; N, trisnapthyl; and P, hexaphenyl derivatives of cyclotriphosphazatriene.

revealed at 1408 cm^{-1} (Table 1), agrees with partial substitution of the chlorine atoms in the fluorene derivative (Scheme 1) and with the results of the elemental analysis.

UV spectra

The UV spectra (Table 2) are consistently dominated by an intense absorption at 221 ± 15 nm and a less intense band at 261 ± 5 nm. The former is attributed to the phosphazene higher dipole $\pi \rightarrow \pi^*$ transition, whereas the latter less intense band is attributed to the aryl $\pi \rightarrow \pi^*$ transition. It is important to recognize that the phosphazene ring transition is much more intense for all the aryl derivatives than for the chloro derivative, which may be due to the higher dipole transition of the protonated phosphazene ring in the former cases. The bathochromic shift (Table 2) observed in this transition follows the same order of increased molecular resonance, which is shown above. This order is also followed systematically by the aryl ring $\pi \rightarrow \pi^*$ transition, except for the fluorene derivative which shows a considerably higher shift. This might be attributed to its coplanar ring structure (Scheme 1, F) which is not possible for the other aryl derivatives (Scheme 1, B, N and P), see below.

TABLE 2

UV band wavelength (nm) and assignment [a] (390–190 nm) of the cyclotriphosphazatriene derivatives

	Derivatives of cyclotriphosphazatriene				
	Phenyl	Biphenyl	Naphthyl	Fluorene	Chloro
Phosphazene $\pi \rightarrow \pi^*$	236	223	216	206	204
Aryl $\pi \rightarrow \pi^*$	266	260	256	285	

[a] Band assignment is made as based on spectral correlation with previously published relevant data [13, 14].

^{1}H-NMR spectra

The ^{1}H-NMR spectra (Table 3) consistently show two broad resonances: the higher field resonance is attributed to the phosphazene N^+H, and the lower field resonance to the more deshielded aryl C–H protons. In addition, the fluorene derivative shows a mid-field resonance at 4.2 ppm for the cyclic free C–H proton. This agrees with the IR spectral contribution at 1408 cm^{-1} assigned to the cyclic free in-plane C–H bending. The chemical shift of the former common resonances (Table 3) is influenced by the same order of increased molecular resonance: phenyl > biphenyl > napthyl > fluorene.

The fluorene derivative, although characterised by the lowest molecular resonance, shows a higher chemical shift of 4.2 ppm (as compared with 3.8 ppm for the parent fluorene) for the cyclic free C–H proton. This is considered as confirming the increased molecular resonance in these phosphazene compounds.

The order of increased molecular resonance, which is revealed consistently by the various tools of molecular spectroscopy, is important in the discussion below of the thermal features and shifts observed in these compounds.

TABLE 3

^{1}H-NMR chemical shift (ppm) and assignment (0–15 ppm) of the cyclotriphosphazatriene derivatives

	Polycyclic aryl derivative of cyclotriphosphazatriene			
	Phenyl	Biphenyl	Naphthyl	Fluorene
Phosphazene N^+–H	3.40	2.50	2.40	2.30
Cyclic C–H				4.20
Aryl protons	7.70	7.55	7.50	7.40

Differential thermal analysis

Except for the fluorene derivative, whose thermogram shows only an endothermic solid–liquid phase transition, the aryl derivatives reveal an

TABLE 4

DTA of the cyclotriphosphazatriene derivatives

Aryl derivative	Solid–solid phase transition			Solid–liquid phase transition		
	T_c/K	H/(J g^{-1})	E^*/(kJ g^{-1} K^{-1})	T_c/K	H/(J g^{-1})	E^*/(kJ g^{-1} K^{-1})
Phenyl	438	7.45	220	510	8.62	602
Biphenyl	403	5.96	161	473	4.79	366
Naphthyl	388	5.48	115	465	4.46	261
Fluorene				393	3.50	143

additional solid–solid phase transition at lower T_c values. The transition T_c (Table 4) and C_p values, whether of the solid state (Fig. 3) or solid–liquid (Fig. 4) transition, increase in the order revealed by the preceding spectral analyses.

It is important to point out that despite the strict dependence of the T_c on the molecular structure, an almost equal temperature rise of 70 K (Table 4) is required to cross the energy gap separating the two phase transitions.

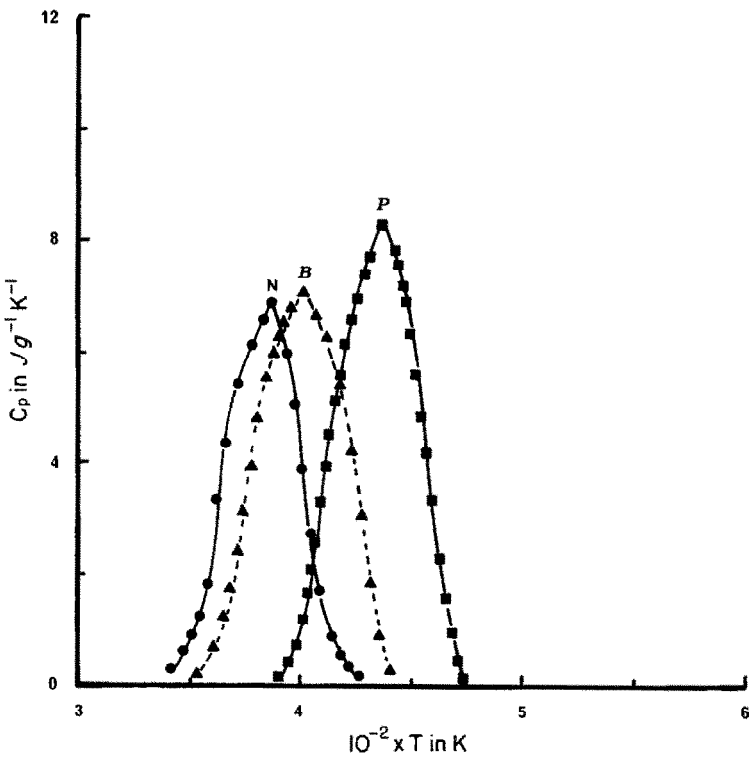

Fig. 3. Dependence of the specific heat of the solid state phase transition on temperature. Symbols as in Fig. 1.

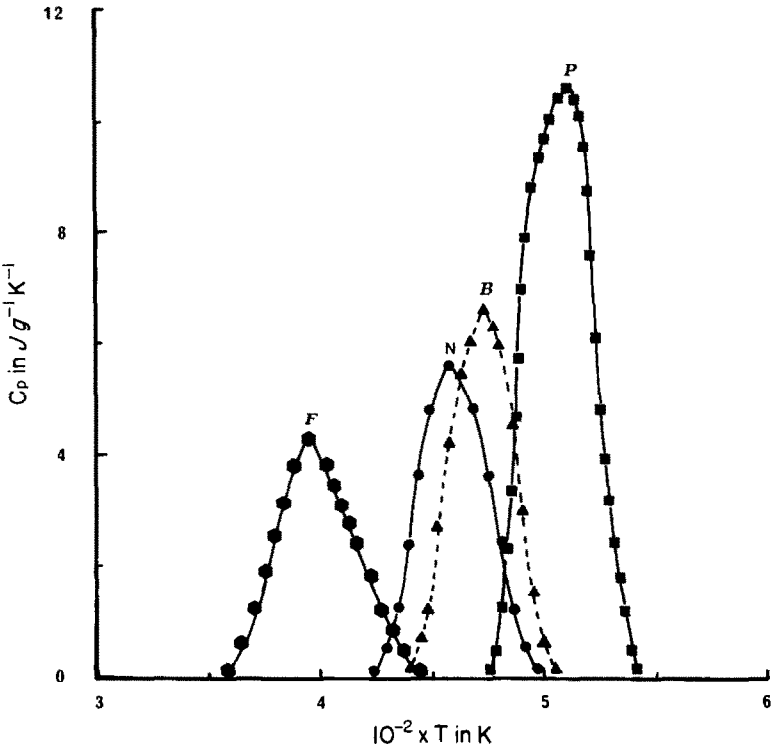

Fig. 4. Dependence of the specific heat of the solid–liquid phase transition on temperature. Symbols as in Fig. 1.

This would indicate a similar route of thermal activation to the molten state for all the aryl derivatives, except for the fluorene derivative which, as for the hexachloro derivative, shows no solid state phase transitions. As noted above, the fluorene compound also shows no evidence of a protonated phosphazene. This, together with the absence of a solid state phase transition, would assign both the solid state phase transition and the temperature gap of 70 K to the thermal activation required for cleaving the intramolecular association found in the other aryl derivatives. The transition C_p (Figs. 3 and 4) and T_c (Table 4) values follow the established order of increased molecular resonance and intramolecular association evident in the preceding spectral analysis.

The enthalpy change ΔH of the transition is calculated with reference to the solid state transition of pure indium (28.4 J g^{-1}) at 703 K. The calculated values (Table 4), although they are relatively low, reflect the same order shown above. The relatively low values indicate relatively strained structure, which varies slightly from one derivative to another. The higher enthalpy of the phenyl derivative is, therefore, due to a less strained structure. The intramolecular H-bonding, which associates the protonated

phosphazene N^+–H with the aryl ring π-bonding electrons, should increase with the ring basicity which, in turn is related to the molecular resonance. Such a strong intramolecular association assists in stabilising the molecular structure against strain in such polycyclic compounds. Stronger intramolecular association is accommodated more favourably in the phenyl derivative than in the biphenyl derivative, than in the naphthyl derivative. The more associated phenyl derivative has the least strained structure (Scheme 1, P) and shows the highest enthalpy transitions (Table 4). Bonding the geminally substituted phenyl rings together, as in the biphenyl derivative (Scheme 1, B), strains the molecular structure so that lower association and enthalpy are shown. This is shown to a more pronounced extent for the fused naphthyl ring structure (Scheme 1, N). However, the non-associated fluorene derivative, due to the coplanar structure (Scheme 1, F), has the highest strained structure and shows the least enthalpy transition.

The activation energy of the transition E^* is calculated from the logarithmic dependence

$$\ln(C_p T^2) = \ln(ZNU^2/R) - E^*/RT$$

where Z is a coordination number, N the number of defects, R the universal gas constant and E^* the activation energy. E^* is best calculated far from the transition T_c and near the early stage of the propagation of the transition [15]. Figure 5 correlates such a linear dependence of C_p on T for the solid state phase transition, where a consistent order of the T_c and E^* values is

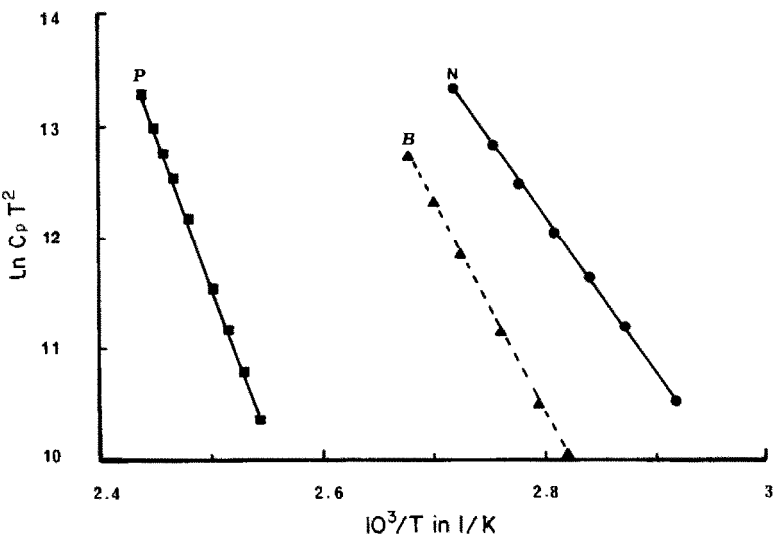

Fig. 5. Arrhenius-like dependence of the specific heat of the solid state phase transition on temperature. Symbols as in Fig. 1.

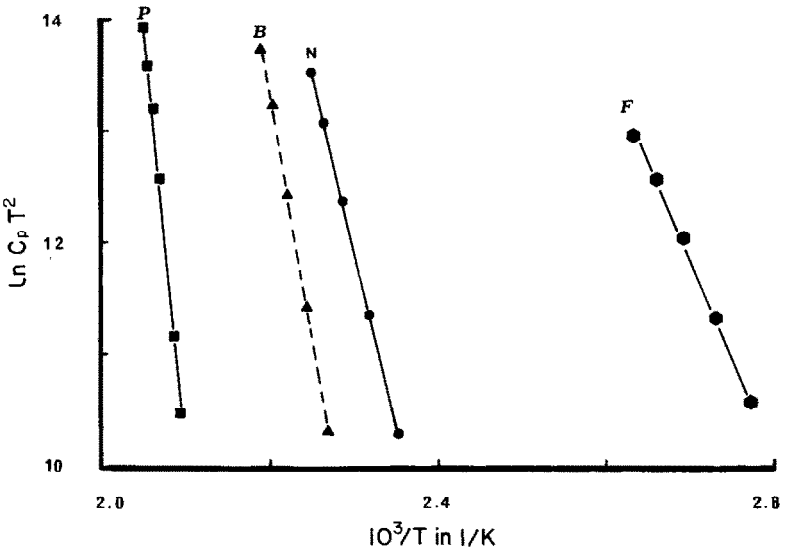

Fig. 6. Arrhenius-like dependence of the specific heat of the solid–liquid phase transition on temperature. Symbols as in Fig. 1.

revealed. A similar dependence (Fig. 6) is shown by the solid–liquid phase transition. This would support and confirm the established order shown above.

The agreement shown by these various thermodynamic parameters, particularly when supported by various spectral evidence, suggests that although the structural differences in the present group of compounds are slight, the complementary spectral and thermal analyses have elucidated the various important structural dependencies that could be investigated further by X-ray crystallography.

REFERENCES

1 A.H. Al-Kubaisi and M.B. Sayed, Thermochim. Acta, 222 (1993) 241.
2 M.I. Davis and J.W. Paul, Acta Crystallogr., Suppl. 25A (1969) 5116; J. Mol. Struct., 12 (1972) 249.
3 R.H. Boyd and L. Kesner, J. Am. Chem. Soc., 99 (1977) 4248.
4 J.P. Huvenne, G. Vergoten and P. Legrand, J. Mol. Struct., 63 (1980) 47.
5 P.C. Painter, J. Zarian and M.M. Coleman, Appl. Spectrosc., 36 (1982) 265.
6 M.B. Sayed, M.E. Kassem and I.M. Al-Emadi, Thermochim. Acta, 188 (1991) 143.
7 C.W. Allen, Chem. Commun., (1970) 152.
8 A.C. Chapman and N.L. Paddock, J. Chem. Soc., (1962) 635.
9 J. Emsley and N.L. Paddock, J. Chem. Soc., (1970) 109.
10 R. Keat and R.A. Shaw, in G.M. Koslapoff and L. Maier (Eds.), Organic Phosphorus Compounds, Vol. 6, John Wiley, New York, 1973, p. 833.

11 L.C. Thomas, Interpretation of the Infrared Spectra of Organophosphorus Compounds, Heyden, 1974.
12 L.J. Bellamy, The Infrared Spectra of Complex Molecules, Chapman and Hall, 1975.
13 B. Lakatos, A. Hesz, Z. Vetessy and G. Horvath, Acta Chim. Acad. Sci. Hung., 66 (1969) 309.
14 A.J. Wagner and T. Moeller, J. Inorg. Nucl. Chem., 33 (1971) 1307.
15 D.S. Gaunt and C. Domb, J. Phys. C., Ser. 2(I) (1968) 1038.